

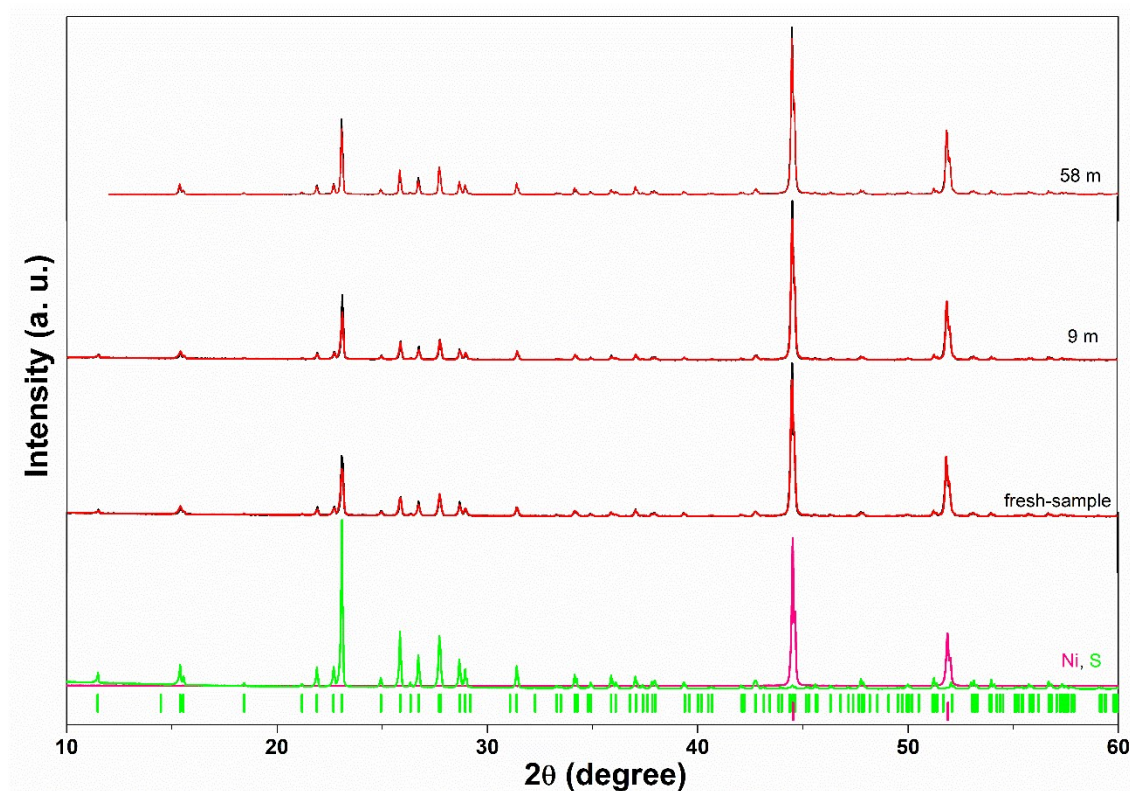
## Supplementary Information

### Synthesis of *n*-hydrated Nickel sulfates from mechanically alloyed nanocrystalline Nickel sulfides

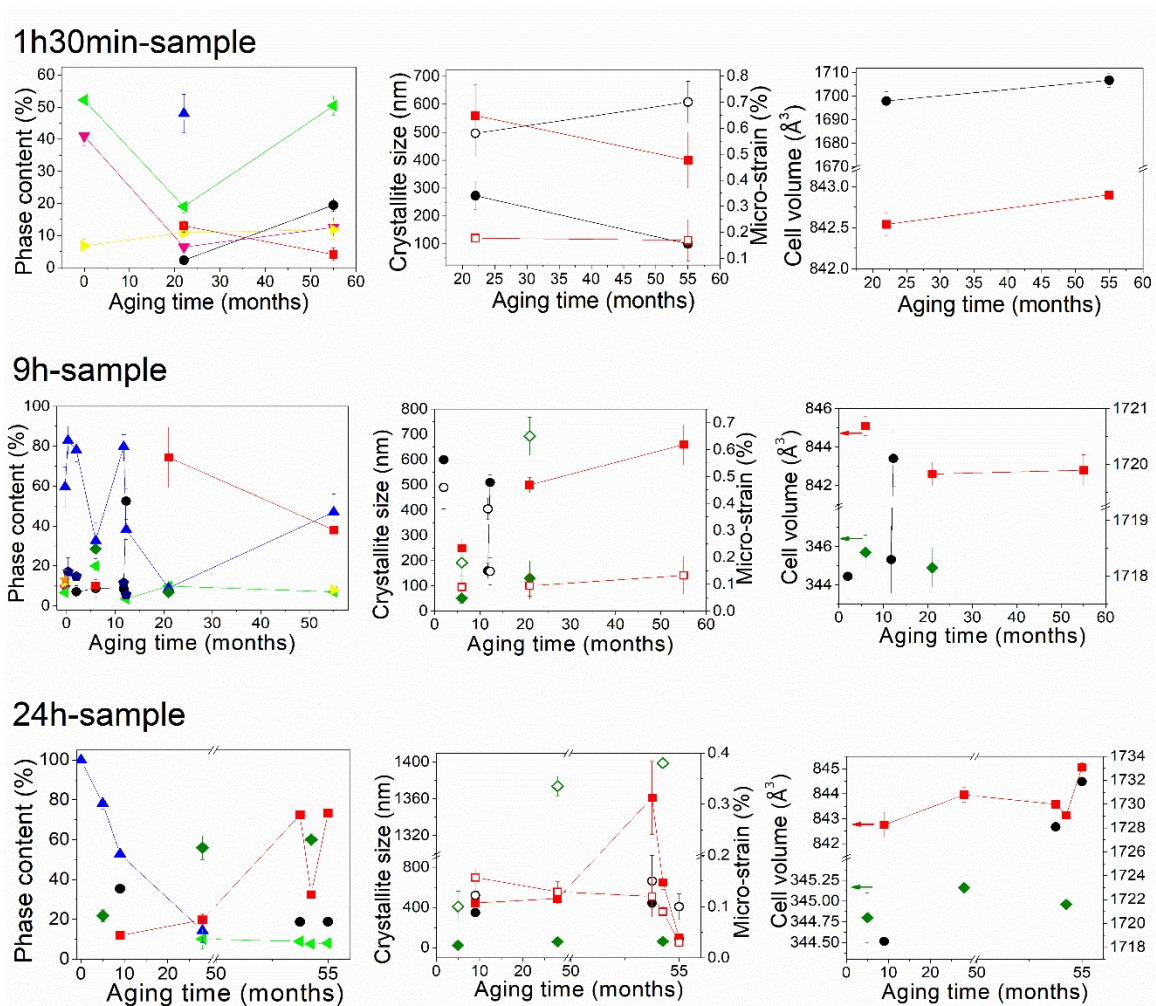
K.F. Ulbrich<sup>1</sup>, B.S. Souza<sup>2</sup>, C.E.M. Campos<sup>1, a</sup>

<sup>1</sup> Departamento de Física, Universidade Federal de Santa Catarina, 88040-970 Florianópolis, Brasil

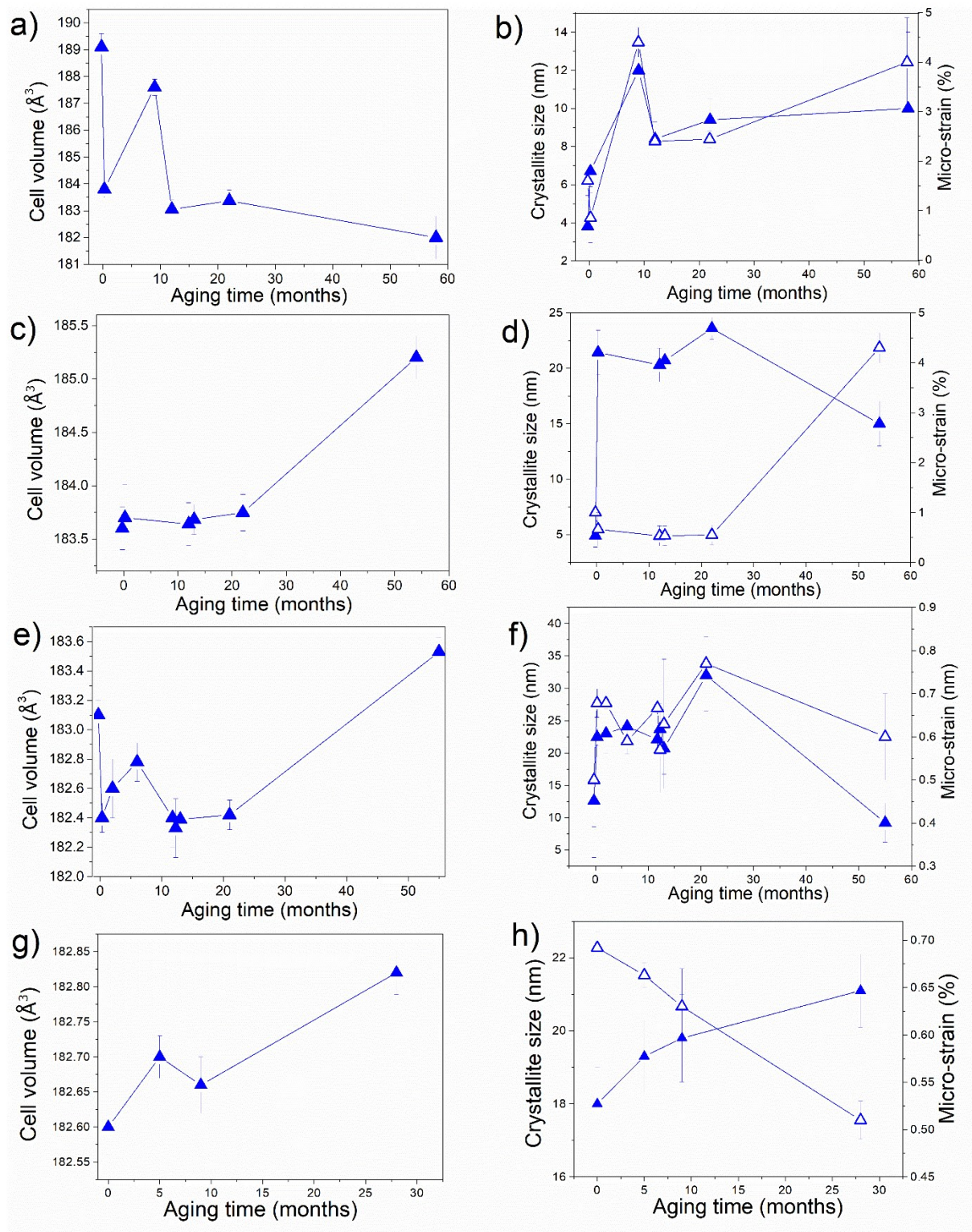
<sup>2</sup> Departamento de Química, Universidade Federal de Santa Catarina, 88040-970 Florianópolis, Brasil



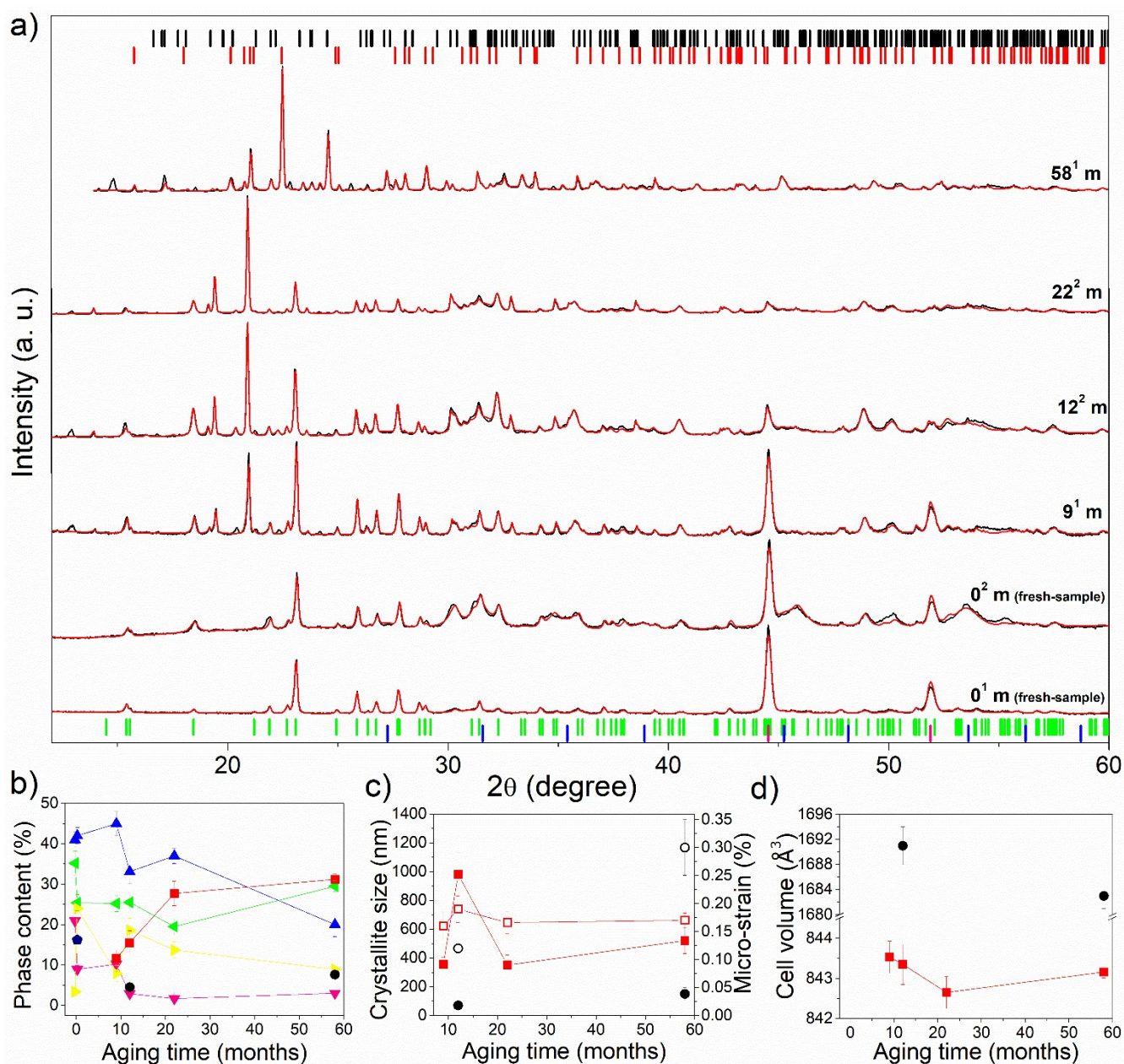
**Fig. S1** (a) XRPD patterns of the mixed powder  $\text{Ni}_{34}\text{S}_{66}$  0h-sample with different aging times (black lines). Calculated-Rietveld patterns are represented by the red lines, the experimental patterns of elemental Ni and S are shown by pink and green lines, respectively, as well as the Ni (ICSD 52265) and S (ICSD 27261) tick-markers.



**Fig. S2** Time evolution of phase content, microstructure parameters and cell volume of the NSH phases of the samples milled 1h30min, 9 h and 24 h. The green, pink, blue, red, yellow, black, dark blue, orange and dark green symbols represent the S, Ni, NiS<sub>2</sub>, α-NSH (ICSD 39420), trigonal NiS (ICSD 40053), β-NSH (ICSD 65018), hexagonal NiS (ICSD 49665), Ni<sub>17</sub>S<sub>18</sub> (ICSD 37164) and NiSO<sub>4</sub>H<sub>2</sub>O (ICSD 27095) phases.



**Fig. S3** Structural and microstructural parameters of the NiS<sub>2</sub> phase to samples with different milling times, (a)-(b) 3 h, (c)-(d) 6 h, (e)-(f) 9 h and (g)-(h) 24 h.



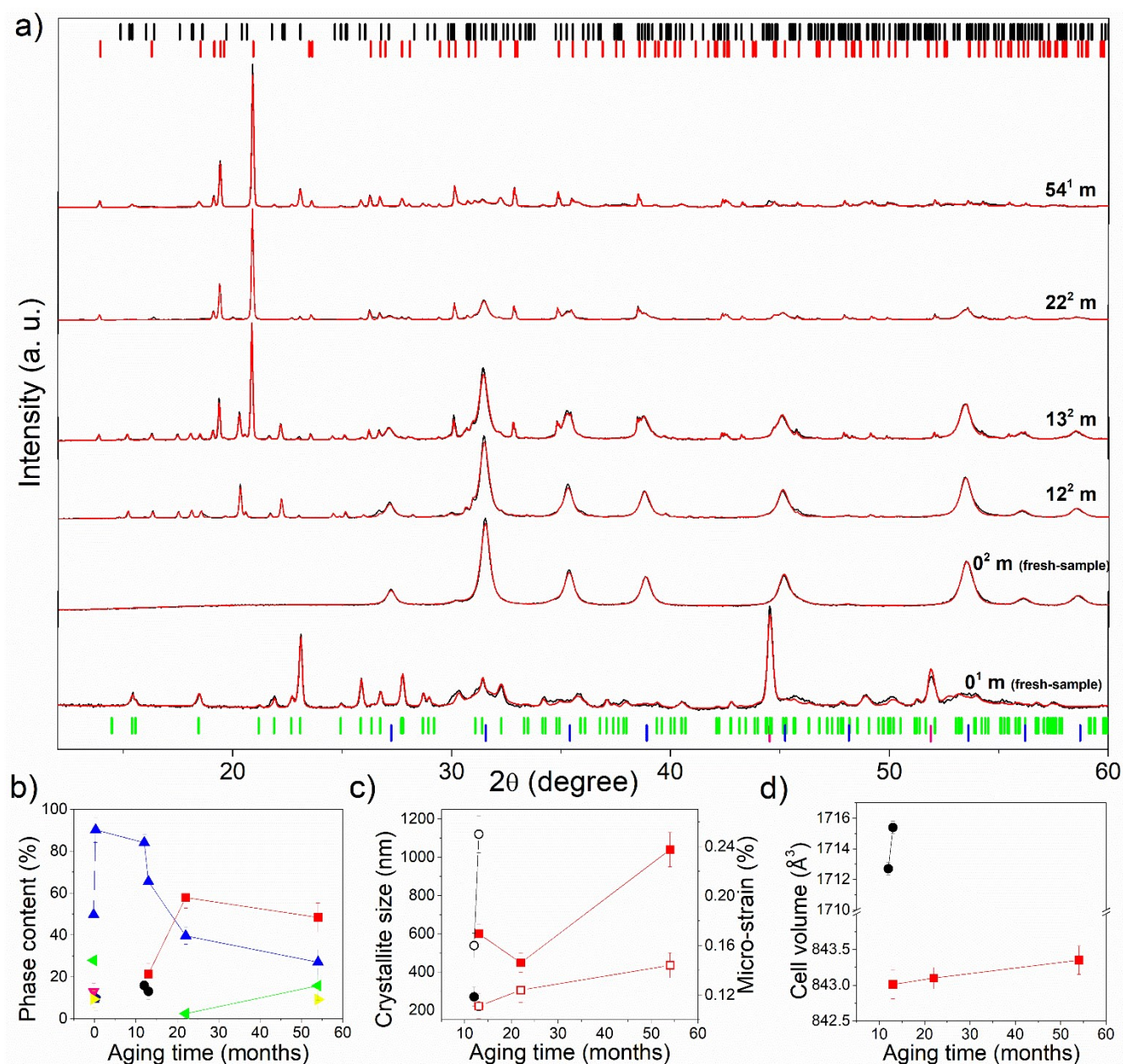
**Fig. S4** (a) Experimental XRPD patterns (black lines) and Rietveld refinement plot (red line) of the  $\text{Ni}_{34}\text{S}_{66}$  milled for 3 h as a function of storage time (aging). The upper indices indicate the preparation condition. Peak markers pink, green, blue, red and black ticks refer to Ni (ICSD 52265), S (ICSD 27261),  $\text{NiS}_2$  (ICSD 166452),  $\alpha$ -NSH (ICSD 39420), and  $\beta$ -NSH (ICSD 65018) respectively. Time evolution of (b) phase fraction, (c) microstructure parameters and (d) cell volume of the NSH phases. The green, pink, blue, red, yellow, black and dark blue symbols represent the S, Ni,  $\text{NiS}_2$ ,  $\alpha$ -NSH, trigonal NiS (ICSD 40053),  $\beta$ -NSH and hexagonal NiS (ICSD 49665) phases.

Fig. S4(a) shows the Rietveld fitting of experimental XRPD data of the  $\text{Ni}_{34}\text{S}_{66}$  composite after 3 h of milling and aged up to 58 months. The fresh samples from 1<sup>st</sup> and 2<sup>nd</sup> condition are similar, however, 2<sup>nd</sup>

condition has lower amounts of reagents Ni (8.9%) and S (25.4%), and show the hexagonal NiS (16.2%) phase formation (Fig. S4(b)). Both conditions present the formation of the NiS<sub>2</sub> phase with average crystallite size of 3.8 nm (micro-strain = 1.6%) and 6.7 nm (micro-strain = 0.85%) to 1<sup>st</sup> and 2<sup>nd</sup> conditions (see Fig. S3(b)), respectively, revealing very small crystalline domains with high micro-strain degree. The cell volume of the NiS<sub>2</sub> phase is very different, 189.1 Å<sup>3</sup> to 1<sup>st</sup> condition and 183.8 Å<sup>3</sup> to 2<sup>nd</sup> condition (Fig. S3(a)), indicating that the highest BPR used in 2<sup>nd</sup> condition provides a high compressive stress.

The aging of these samples (Fig. S4(b)), shows that the β-NSH phase appears in a small amount (4.5%) in sample aged 12 months (2<sup>nd</sup> condition) while that aged 22 and 58 months exhibited the largest amount of α-NSH phase (almost 30%), and elemental powders Ni and S tends to decrease. After mechanochemistry process on Ni<sub>34</sub>S<sub>66</sub> composite, the reagents and nickel sulfides phases decreasing provides the growth and increase of the α-NSH phase with aging time.

The samples aged shows average crystallite size of about 100 nm and micro-strain greater than 0.10% to β-NSH phase (see Fig. S4(c)). The α-NSH phase has an average crystallite size between 350 and 980 nm and micro-strain of about 0.17%, revealing large crystals with low crystalline disorder. The cell volume to α-NSH phase shown in Fig. S4(d) tends to decrease with aging, showing that the phase is under a compressive stress.



**Fig. S5** (a) Experimental XRPD patterns (black lines) and Rietveld refinement plot (red line) of the  $\text{Ni}_{34}\text{S}_{66}$  milled for 6 h as a function of storage time (aging). The upper indices indicate the preparation condition. Peak markers pink, green, blue, red and black ticks refer to Ni (ICSD 52265), S (ICSD 27261),  $\text{NiS}_2$  (ICSD 166452),  $\alpha$ -NSH (ICSD 39420), and  $\beta$ -NSH (ICSD 65018) respectively. Time evolution of (b) phase fraction, (c) microstructure parameters and (d) cell volume of the NSH phases. The green, pink, blue, red, yellow, black and dark blue symbols represent the S, Ni,  $\text{NiS}_2$ ,  $\alpha$ -NSH, trigonal NiS (ICSD 40053),  $\beta$ -NSH and hexagonal NiS (ICSD 49665) phases.

The diffraction pattern of the sample after 6 h of milling of the 1<sup>st</sup> condition (Fig. S5(a)) still show the presence of reagents (Ni = 13% and S = 28%) and the  $\text{NiS}_2$  phase was quantified by 50% (and trigonal

NiS = 9%) having very small crystals, of about 5 nm, and high micro-strain (Fig. S3(d)). However, the sample milled 6 h of the 2<sup>nd</sup> condition shows 90% of the NiS<sub>2</sub> phase, with average crystallite size of 21.4 nm and 0.66% of micro-strain, and only 10% of hexagonal NiS (with 14.5 nm and micro-strain of the 0.9%). Here, it is evident that using a higher BPR the reaction becomes faster, i.e., the reagents are consumed more quickly forming the desired phase, and the hexagonal NiS phase formation reaction is favored.

One year after its production, the sample from 2<sup>nd</sup> condition stored inside of microtube shows that the NiS<sub>2</sub> and hexagonal NiS phases are partially converted in the phase  $\beta$ -NSH, about 16% (Fig. S5(b)) with average crystallite size of 270 nm, micro-strain of 0.16% and cell volume of the 1712.7 Å<sup>3</sup> (see Fig. S5(c-d)). Therefore, as seen for samples milled 1h30min and 3 h, the reagents and nickel sulfides phases decrease provides the growth and increase of the  $\alpha$ -NSH phase with aging time. After one month of exposure to air during the XRPD measurement, this same sample, showed a large increase in amount of the nickel sulfate phases almost 116% ( $\beta$ -NSH = 13.1% and  $\alpha$ -NSH = 21.4%) evidencing that the sample exposure is a crucial factor for the appearance of the NSH phases. We observed that the NiS<sub>2</sub> phase tends to decrease with aging and that the  $\alpha$ -NSH phase becomes the most stable phase ( $\beta$ -NSH phase is stable above 50 °C). The samples aged 22 and 54 months exhibited the largest amount of  $\alpha$ -NSH phase about 60%.

Up to 22 months of aging, the NiS<sub>2</sub> phase does not undergo major changes in its structure and microstructure, however, for 54 months of aging the sample produced in the 1<sup>st</sup> condition shows a large increase in the crystallite size (Fig. S3(d)), again indicating the probable transformation of the smaller crystals (firstly) to NSH phases. The NSH phases has an average crystallite size between 250 and 1000 nm depending on the condition and low micro-strain (see Fig. S5(c)). Cell volume (Fig. S5(d)) shows a slight increase for both NSH phases indicating that the phases are under a distensile stress.

## Solid state synthesis under ambient atmosphere

Starting mixtures of nickel (Sigma-Aldrich 99.99%) and sulfur (Sigma-Aldrich 99.997%) high-purity powders with nominal composition of  $\text{Ni}_{34}\text{S}_{66}$  and  $\text{Ni}_{50}\text{S}_{50}$  were ball milled under ambient atmosphere up to 21 h using a SPEX 8000D Mixer/mill (working at 1425 rpm) high energy ball mill. The powders were mixed in a 65 mL cylindrical stainless steel container with nine stain steel balls (three with an average diameter of 12.7 mm and six with an average diameter of 6.35 mm), for  $\text{Ni}_{34}\text{S}_{66}$  composition 4% distilled water was add in the powder mixture. The ball-to-powder weight ratio was 10:1. The synthesis of the samples was stopped every third hour to fish out a small portion of the sample for ex-situ characterization. After nine hours of synthesis the set of smaller balls were exchanged in order to avoid deformation of the balls and consequently contamination of the reaction.

## Results

Fig. S6(a) shows the XRPD patterns of the  $\text{Ni}_{34}\text{S}_{66}$  samples with different milling times. Initially, formation of  $\text{NiS}_2$  and  $\text{NiS}$  phases was observed, along with about 2% Fe (Fig. S6(b)). The Fe comes from the wear of the milling tools due to the absence of inert atmosphere during synthesis, thus, in this condition the reaction becomes more abrasive to milling tools. For longer milling times, Fe reacts with oxygen forming the  $\text{Fe}_3\text{O}_2$  phase. In the 15h-sample 2.3% of  $\beta$ -NSH was identified (crystallite size of about 300 nm and micro-strain of 0.13%). The XRPD patterns of the  $\text{Ni}_{50}\text{S}_{50}$  samples with different milling times, Fig. S7(a), shows the hexagonal  $\text{NiS}$  phase formation, presence of Fe (from milling tools wear) and  $\text{Fe}_2\text{NiO}_4$  phase formation was identified after 12 h of milling.

After milling the samples were stored inside of microtubes and a small portion of the samples milled for 21 h were stored in an improvised humidifier (as shown in Fig.S8) for almost 1 month (and then returned to microtube) in order to accelerate the NSH formation process and were named of damp samples. The aged samples were analyzed by XRPD and results are shown in Figs. S9 and S10. The  $\text{Ni}_{50}\text{S}_{50}$  aged samples (Fig. S9) inside of microtubes did not shows the NSH phases formation, but the sample that remained in the humidifier presented 24.5%, and after 5 month this amount increasing to 35%, indicating that a more humid ambient, i.e., with a higher content of water, is more favorable for the formation of NSH phases. However, the samples stored inside of microtubes of the composition  $\text{Ni}_{34}\text{S}_{66}$  showed a large amount of the sulfate phases, reaching up to 26% of  $\alpha$ -NSH for the 15h-sample aged three months (that had presented 2.3% of  $\beta$ -NSH in the milling). The NSH phases are formed from nickel sulfides since the amount decreases, while the amount of the Fe and  $\text{Fe}_2\text{O}_3$  phases remains unchanged. The greatest amount of NSH phase was obtained in the 21h-sample damp aged 5 months, almost 46% of  $\alpha$ -

NSH phase and 7.4% of  $\beta$ -NSH are present. Therefore, keeping the samples in an ambient with high humidity directly accelerates the formation of the  $\alpha$ -NSH phase.

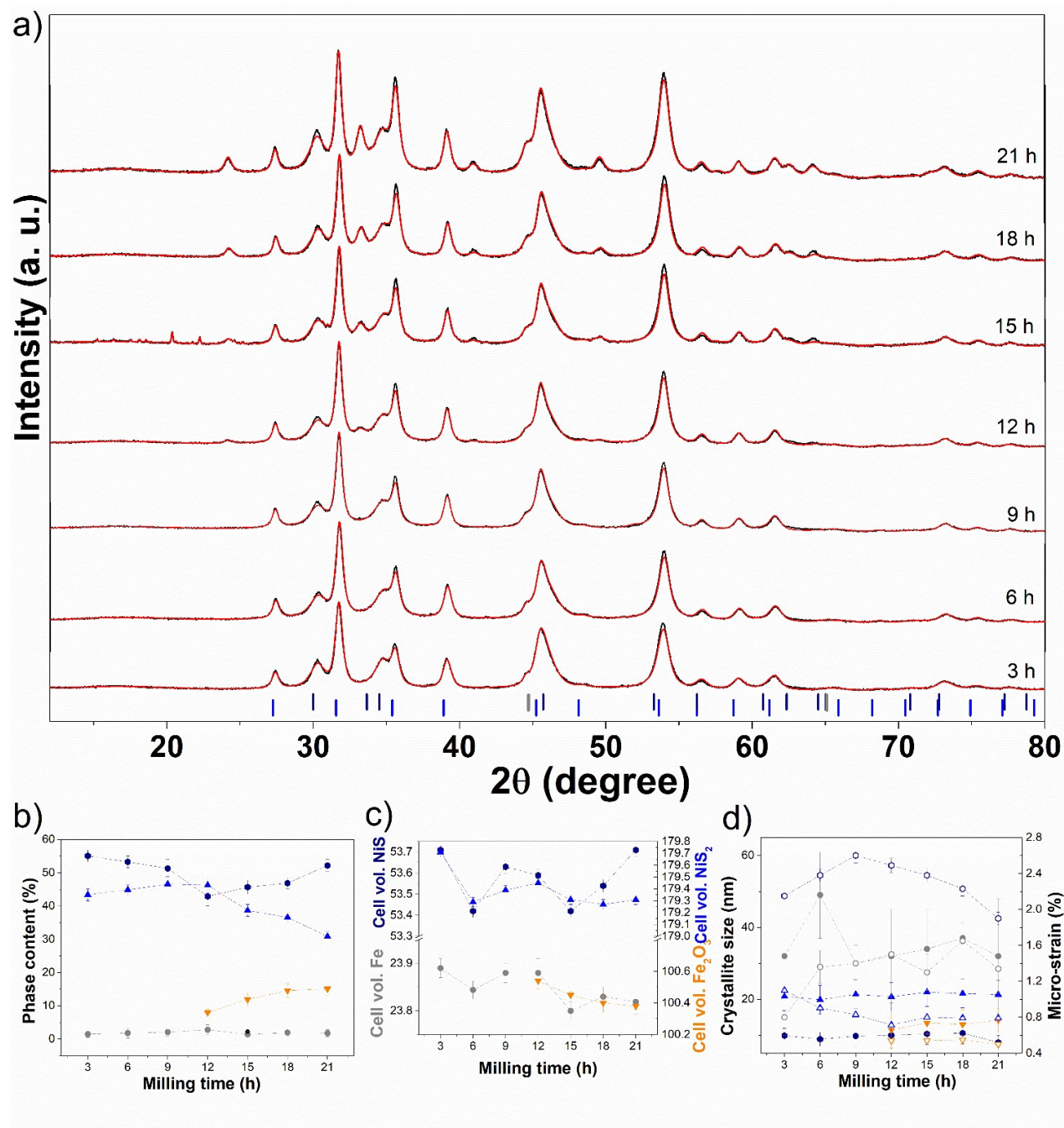


**Fig. S6** (a) XRPD of  $\text{Ni}_{34}\text{S}_{66}$  with different milling times. Rietveld refinement plot (red line) and peak markers blue, dark blue and gray ticks refer to  $\text{NiS}_2$  (ICSD 166452),  $\text{NiS}$  (ICSD 49665) and  $\text{Fe}$  (ICSD 53802), respectively. (b) Phase fraction, (c) cell volume and (d) microstructure parameters (open and closed symbols represent micro-strain and crystallite size, respectively) as a function of milling time. The blue, orange, dark blue and gray symbols refer to  $\text{NiS}_2$ ,  $\text{Fe}_2\text{O}_3$ ,  $\text{NiS}$  and  $\text{Fe}$  phases.

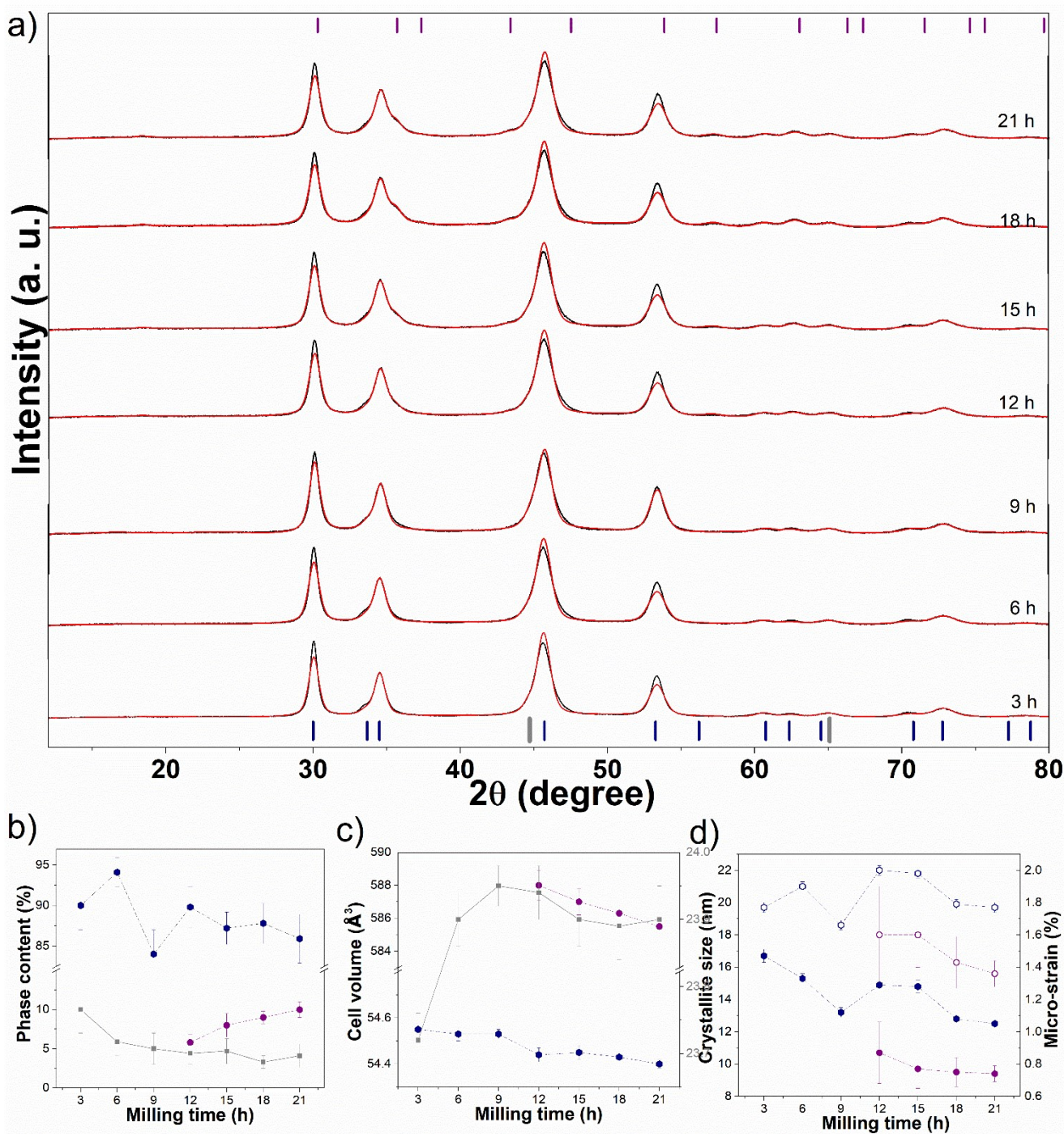


**Fig. S7** (a) XRPD of  $\text{Ni}_{50}\text{S}_{50}$  with different milling times. Rietveld refinement plot (red line) and peak markers dark blue, purple and gray ticks refer to NiS (ICSD 49665),  $\text{Fe}_2\text{NiO}_4$  (ICSD 28108) and Fe (ICSD 53802). (b) Phase fraction, (c) cell volume and (d) microstructure parameters (open and closed symbols represent micro-strain and crystallite size, respectively) as a function of milling time. The dark blue, purple and gray symbols refer to NiS,  $\text{Fe}_2\text{NiO}_4$  and Fe phases.



**Fig. S8** Improvised humidifier using a desiccator containing water at the bottom and the samples on the glass disc.

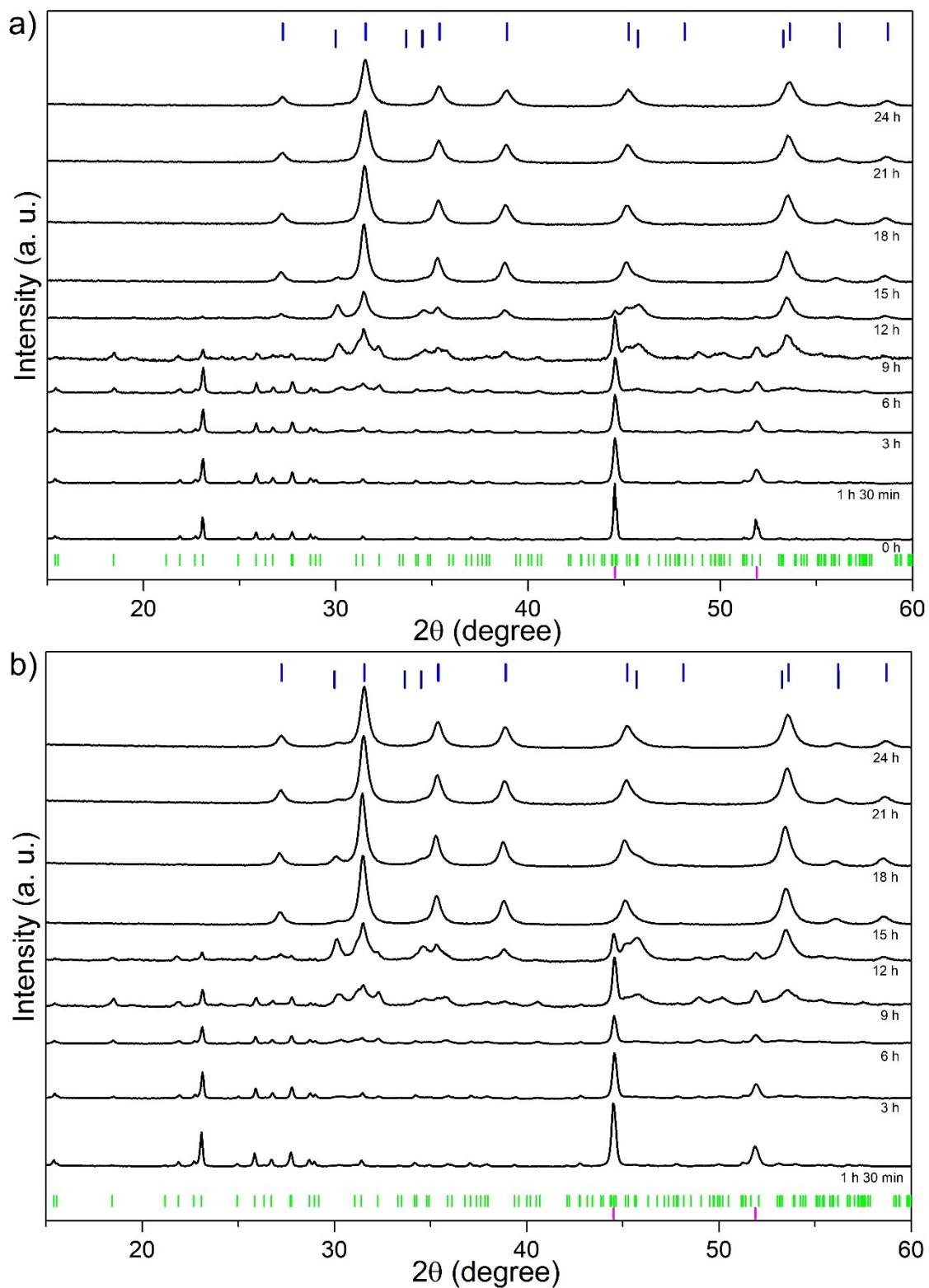


**Fig. S9** XRPD patterns (black lines) of  $\text{Ni}_{34}\text{S}_{66}$  with different milling times (a) first and (b) second batch. Peak markers blue, dark blue, pink and green refer to  $\text{NiS}_2$  (ICSD 166452),  $\text{NiS}$  (ICSD 49665),  $\text{Ni}$  (ICSD 52265) and  $\text{S}$  (ICSD 27261), respectively.

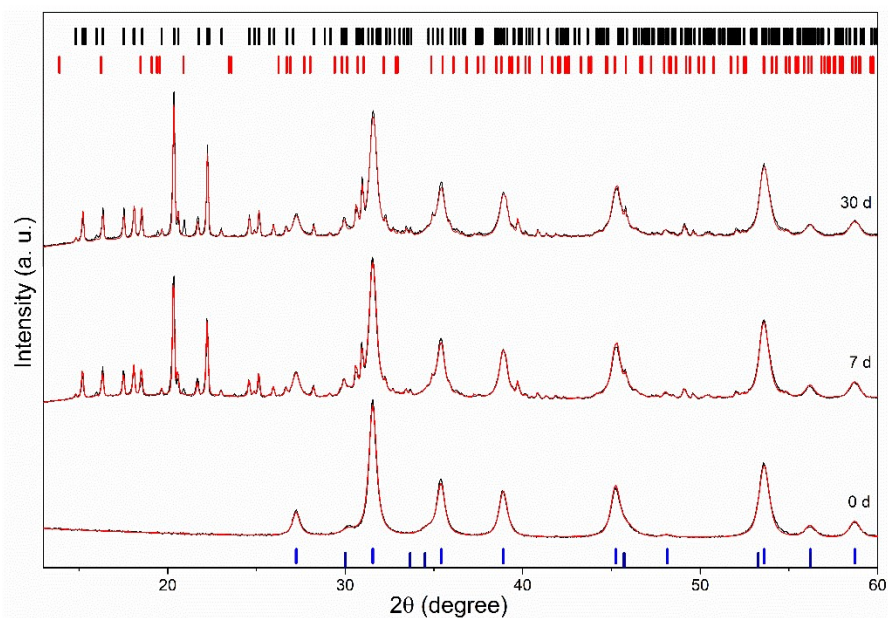
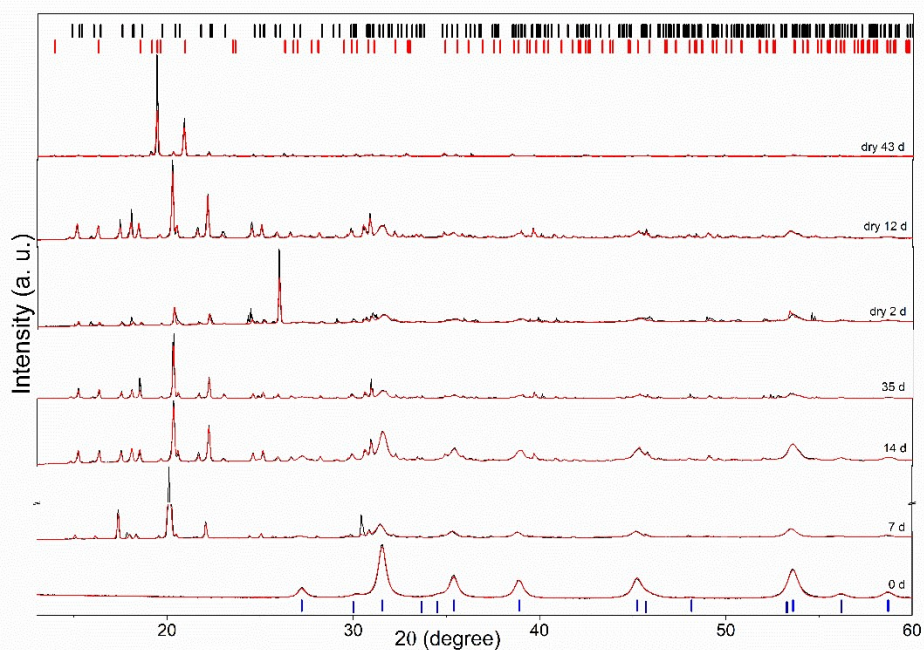


**Fig. S10** XRPD patterns (black lines) and Rietveld refinement plot (red lines) of the  $\text{Ni}_{34}\text{S}_{66}$  24 h of milling with different aging times at ambient conditions. The blue, red, black and dark blue peak markers represent the  $\text{NiS}_2$  (ICSD 166452),  $\alpha\text{-NSH}$  (ICSD 39420),  $\beta\text{-NSH}$  (ICSD 65018) and hexagonal  $\text{NiS}$  (ICSD 49665) phases.



(ICSD 49665) phases.

**Fig. S11** XRPD patterns (black lines) and Rietveld refinement plot (red lines) of the  $\text{Ni}_{34}\text{S}_{66}$  24 h of milling with different aging times at temperature ambient and high humidity. The blue, red, black and

dark blue peak markers represent the NiS<sub>2</sub> (ICSD 166452), α-NSH (ICSD 39420), β-NSH (ICSD 65018) and hexagonal NiS (ICSD 49665) phases.

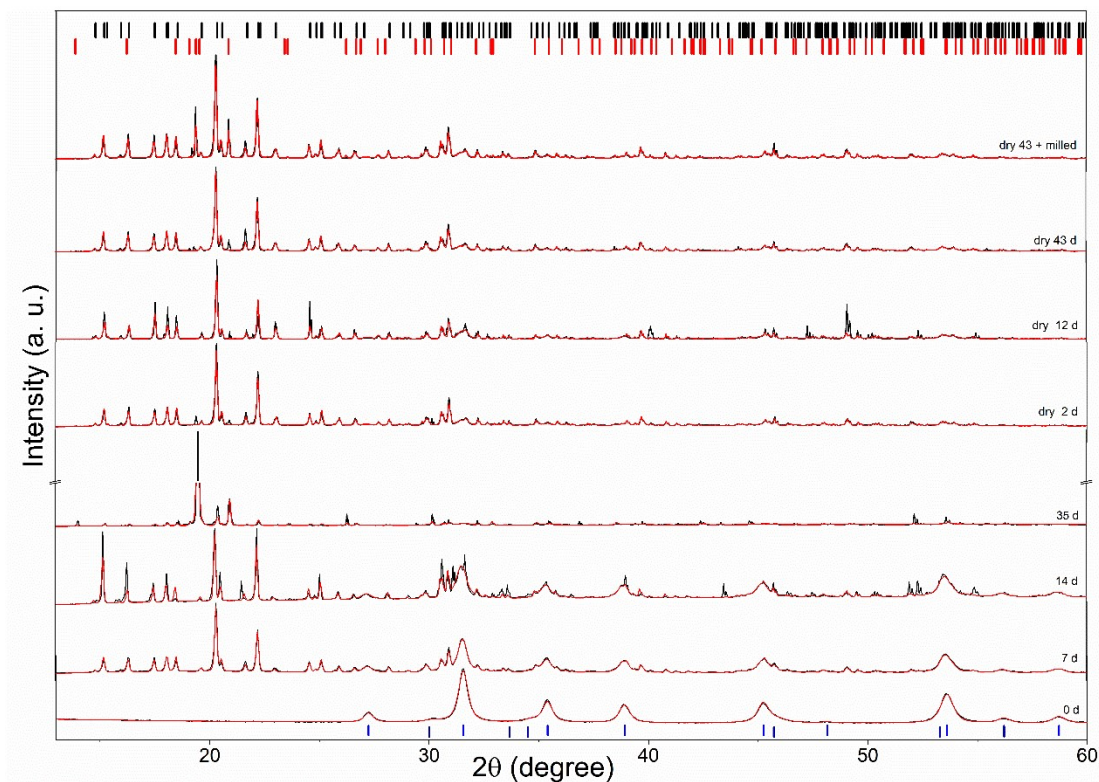


**Fig. S12** XRPD patterns (black lines) and Rietveld refinement plot (red lines) of the Ni<sub>34</sub>S<sub>66</sub> 24 h of milling with different aging times at 50 °C and high humidity. The blue, red, black and dark blue peak markers represent the NiS<sub>2</sub> (ICSD 166452), α-NSH (ICSD 39420), β-NSH (ICSD 65018) and hexagonal NiS (ICSD 49665) phases.

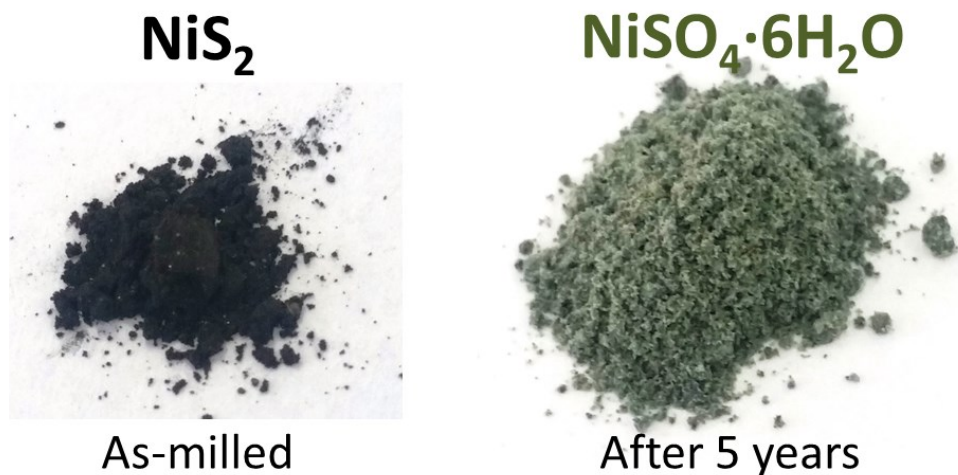


**Fig. S13** Ni<sub>34</sub>S<sub>66</sub> 24 h of milling (left) as-milled and (right) after 5 years.

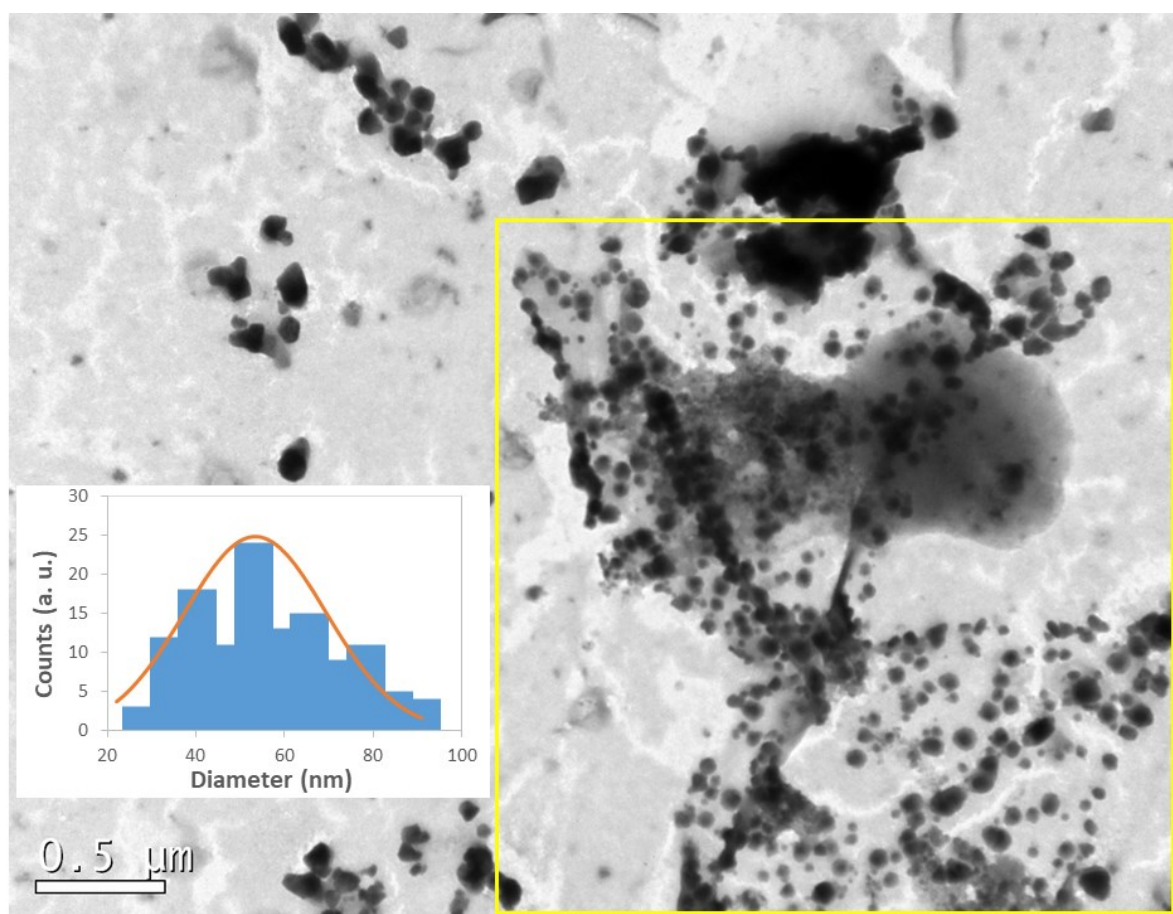


**Fig. S14** TEM image of Ni<sub>34</sub>S<sub>66</sub> 24h aged about 5 years and corresponding nanocrystal size distribution histogram.

## **Metrics calculation, EcoScale**

Considering:

Nickel (100 g, 99,99% purity, 88.00 USD) and Sulfur (250 g, 99,998% purity, 267.00 USD) from Sigma-Aldrich.